On the formation and evolution of nanoscale water condensates in scanning probe microscopy

Vincent Fokkema

On the cover:

Top: The graphite surface with water condensates, as measured with the atomic force microscope.
Bottom: Part of of the used atomic force microscope (Digital Instruments). The graphite sample and the position where the tip is mounted are visible.

On the formation and evolution of nanoscale water condensates in scanning probe microscopy

Vincent Fokkema

August 2006

Abstract

Starting from the observation, that in friction force microscopy the presence of water vapor could lead, through capillary condensation between tip and sample, to ice formation at room temperature on the probed graphite substrate, we continued this line of research to further explore the physical properties of this phenomenon. We used an atomic force microscope, in a controlled environment, to create these nanometer sized condensates in a similar fashion. The versatility of the atomic force microscope allowed us to image the result without perturbing the condensates and hence to study their evolution in space and time. To our surprise, the lifetime of the condensates was much larger than anticipated from the experiment that arose our curiosity; theoretical considerations did not support either observation. To our mischief the conducted experiments showed uncontrolled, unrepeatable behavior. This hindered a rigorous analysis of the data and hence, of further theoretical understanding. We present various experimental cases leading to a kaleidoscopic view of the phenomena. To our opinion there is ample evidence of a structural irregularity in the formation and evolution of the condensates, justifying further investigation.

Contents

Chapter 1

Introduction

With the invention of the scanning tunnelling microscope (STM) [1] and the atomic force microscope (AFM) [2] it became possible to investigate the properties of surfaces on the atomic scale. With friction force microscopy (FFM), a derivative of AFM, friction on the atomic scale is probed. A fundamental understanding hereof is of practical importance to for instance the mechanical properties of micro-electro-mechanical systems (MEMS), of which the moving parts are subject to wear due to friction, leading to their breakdown [3]. Water, present under normal operating conditions, can enhance the friction because adhesion forces between the moving parts add to the normal load, on which the friction is dependent. In FFM, it has been shown that the formation of a capillary water bridge between the scanning probe and the scanned surface influences the friction force [4, 5], depending on the circumstances it may either increase or decrease the friction.

This thesis reflects the work done in the Interface Physics group of the Leiden Institute of Physics in the period from October 2005 to June 2006. The influence of the presence of water in scanning probe microscopy (SPM) is studied.

The direct onset of our research lies in the observations done by K. B. Jinesh *et al.* [6] with the Tribolever™ [7], a home-built, high resolution friction force microscope. With this technique the influence of relative humidity on nanoscale friction on graphite was studied, using a tungsten probe. The researchers found that under particular circumstances (scan velocity, scan size), at high humidity, the friction loops[1] measured showed peculiar behavior, as shown in Figure 1.1. The scenario, proposed to explain the observations, is described in Figure 1.2. From this, and from the actual lateral force it is argued that capillary condensation allows for the formation of a condensate that exhibits the properties of ice rather than liquid water, i.e. the elastic modulus, the maximum shear stress and the

[1] A friction loop shows the friction force as a function of a forward and backward scan, showing static and dynamic friction, as in Figure 1.1.

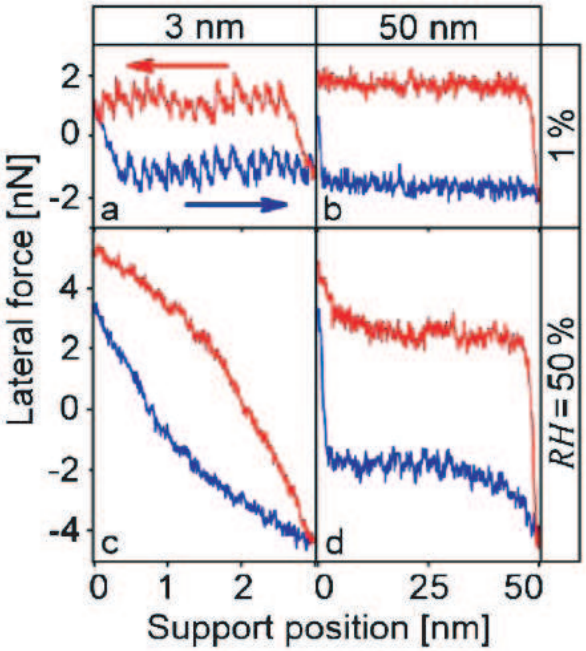

Figure 1.1: Friction loops taken from [6]. At low humidity (a), (b) the tip moves in 'stick-slip' motion over the surface. At higher humidity, the loop is tilted for small scan sizes (c) and for larger scan sizes, peaks are observed at the end of the forward and backward trace (d).

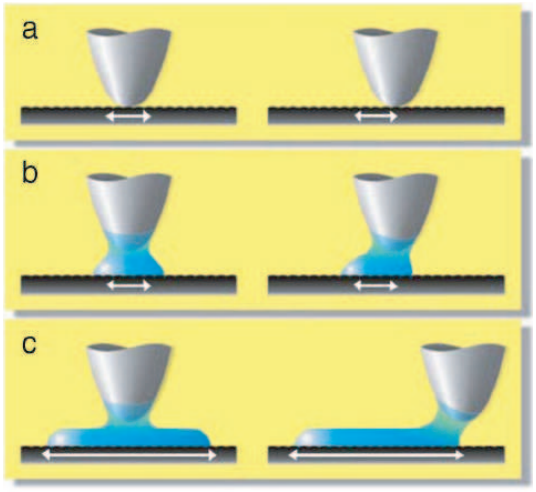

Figure 1.2: The proposed mechanism leading to the observations, depicted in Figure 1.1, taken from [6]. At low humidity the scanning tip directly measures the friction on the graphite atoms (a). At higher humidity capillary condensation occurs and the condensate exerts elastic force on the tip, leading to a tilt in the friction loop for small scan sizes (b). When the scan size is increased more water is condensed but at the end of the trace the condensate still exerts an elastic force on the tip, resulting in a peak in the friction loop (c).

viscosity are much closer to those of ice than those of liquid water. Furthermore, as is indicated in Figure 1.2(c), the condensate proved to be present, for a characteristic time of 2 s, even without the confinement between tip and sample. This implies that the graphite surface alone suffices to sustain the condensate, the presence of the tip providing, through capillary condensation, the nucleation.

The initial goal of our research was to observe the same behavior with a commercial AFM, and in addition to characterize the effects of other materials in a similar experiment. Measuring atomic scale friction on the graphite surface proved to be difficult, even with the present signal to noise ratio. It should have been possible, however, to measure the peaks in the friction loops as in Figure 1.1(d), although no such observations were made. Nevertheless, there is ample evidence that, also in our experiments, the presence of the AFM tip near the sample of our interest, graphite, induced condensation of water. The properties of these condensates are, to say the least, remarkable. The results are given in Chapter 3 and discussed in Chapter 4. At this point we continue with a treatise of the theoretical background.

Chapter 2

Capillary condensation and nanoscale condensates of water

This chapter describes the mechanism of capillary condensation in general, and between a scanning microscope probe and a surface in particular. Then nucleation of droplets, facilitated by capillary condensation is considered.

2.1 Capillary condensation

2.1.1 General aspects

In the presence of water, restricted geometries, such as pores and cracks in a solid, as well as the small gap between a scanning probe and a surface allow for spontaneous condensation of water in such geometries. The surface of the air liquid interface of such a condensate is curved in order to balance the surface energy and pressure. The difference between the pressure inside the condensate and outside, $\Delta P = P^{in} - P^{out}$, is given by the Young-Laplace equation (2.1).

$$\Delta P = \gamma_{LV} \left(\frac{1}{r_1} + \frac{1}{r_2} \right) = \frac{\gamma_{LV}}{r_e} \tag{2.1}$$

Note that $r_{1,2}$ may be valued positive or negative, depending on the curvature being convex or concave, respectively and that r_e is the effective radius of curvature. At constant temperature we have:

$$v_M^{in} dP^{in} = v_M^{out} dP^{out}, \tag{2.2}$$

where v_M is the molar volume. If we assume the vapor to be an ideal gas and that v_M^{in} is much smaller that v_M^{out}, the differential of (2.1) may be written as:

$$d\left(\frac{\gamma_{LV}}{r_e} \right) = \frac{RT}{v_M^{in} P^{out}} dP^{out} \tag{2.3}$$

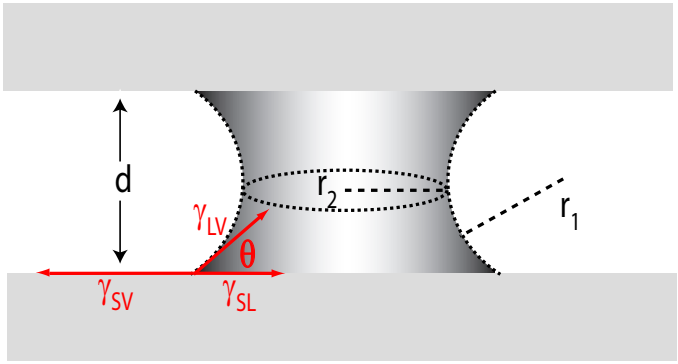

Figure 2.1: Capillary condensation between to parallel plates. The meniscus formed in this example has radii of curvature $r_1 < 0$ (concave) and $r_2 > 0$ (convex), θ is the contact angle with the solid, γ_{SL} is the surface tension of the solid-liquid interface, γ_{SV} is the surface tension of the solid-vapor interface, γ_{LV} is the surface tension of the liquid-vapor interface and d is spacing between the plates.

Integration of (2.3) leads to the well known Kelvin equation [8] (2.4), which couples the equilibrium curvature of the condensate to the relative humidity (RH), P^{out}/P_s and the surface tension of the liquid-vapor interface, γ_{LV}.

$$\frac{1}{r_K} = \frac{RT}{\gamma_{LV} v_M^{in}} \ln\left(\frac{P^{out}}{P_s}\right). \tag{2.4}$$

where r_K is the Kelvin radius, the effective radius satisfying the equilibrium conditions.

A simple example, showing capillary condensation between two parallel plates is given in Figure 2.1. At ambient conditions, $p/p_s < 1$, the capillary neck is stabilized for $r_K < 0$. This implies that $|r_2| > |r_1|$; the meniscus will thus grow until (2.4) is satisfied. The shape and size of the meniscus will furthermore depend on the distance between the plates d and the contact angle with the solid θ. Young's equation (2.5) gives the relation between the contact angle and the surface tensions given in de caption of figure 2.1.

$$\cos\theta = \frac{\gamma_{SV} - \gamma_{SL}}{\gamma_{LV}} \tag{2.5}$$

2.1.2 Capillary condensation at the nanoscale

The theory described above is clearly not applicable to a single molecule, where the meaning of a surface tension is lost. This means that when crossing over from macroscopic to microscopic scales, the validity of the theory of section 2.1.1 is lost. The question remains just at what point this happens. Although one may not speak of surface tension for a single molecule or a small cluster

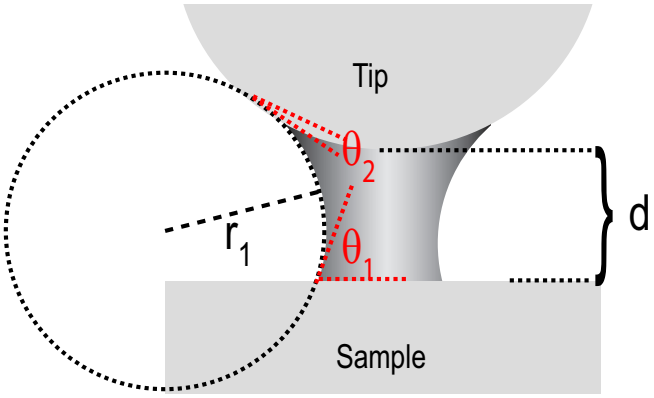

Figure 2.2: Capillary condensation between an AFM-tip and a sample. θ_1 and θ_2 are the respective contact angles of the water-sample interface and the water-tip interface. d is the distance between tip and sample and r_1 is the radius of concave curvature; r_2 is not depicted.

of molecules, there is an energy change associated with transferring molecules from one medium to the other. Concerning this it has been shown [9] that the effective surface tension (energy) of a single molecule or cluster is similar to that of the macroscopic surface, provided that the interaction is of the Van der Waals type.

2.1.3 SiO_2 tip on a graphite surface

Let us now consider the capillary condensation between two objects relevant for our research, namely a atomic force microscopy (AFM) silicon tip (covered by its native oxide) and a graphite surface, see Figure 2.2. In the following we make an explicit calculation, determining the shape and size of the meniscus formed between tip and sample.

The contact angle of water on the silicondioxide tip is 0°, the contact angle on the water-graphite interface is 90°[1]. Figure 2.3 shows the geometry involved in this specific case. Conveniently, the specific contact angles at hand provide the following equation[2], see Figure 2.3:

$$(|r_1| + |r_2|)^2 + (d + r_{tip})^2 = (|r_1| + r_{tip})^2, \tag{2.6}$$

where the absolute values of the radii of curvature are taken, as they can be negatively valued. Together with (2.4), (2.6) determines the size and shape of the capillary condensate.

[1] Actually, the water-graphite contact angle ranges around this value.

[2] The shape and size of the meniscus could be calculated for any given set of contact angles.

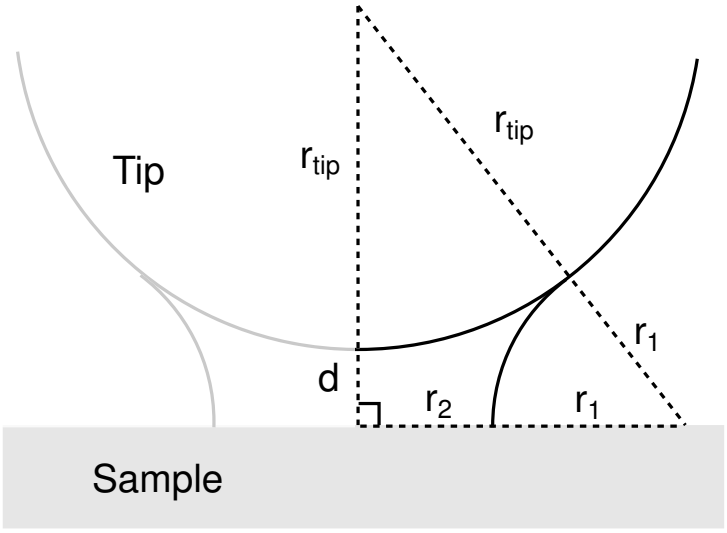

Figure 2.3: The geometry of the water meniscus between tip and sample, with the principle radii of curvature r_1 and r_2, the tip radius r_{tip} and the spacing between tip and sample. d

It is insightful to investigate what is the influence of the relative humidity, the temperature, the spacing d and the tip radius[3] on the formed condensate. Firstly, we consider the effect of the humidity. At a relative humidity of 0%, obviously no capillary condensation occurs. We calculate the principle radii for relative humidity (RH) of respectively 10 %, 50% and 90%, yielding r_K of -0.23 nm, -0.78 nm and -5.1 nm at a temperature of 293 K. For RH of 100 % (2.4) fails, but in the limit the equilibrium shape can be calculated. The spacing d is taken to be 0 nm and the tip radius is chosen to be 10 nm at this instance. Figure 2.4 depicts the equilibrium shape of the meniscus for these values of RH. In the limit of RH $\rightarrow$ 100 %, $r_K \rightarrow -\infty$ the principle radii reach their maximum value of r_1 = -6.7 nm and r_2 = 6.7 nm, for the given tip radius and tip-sample spacing. Figure 2.5 shows a graph of the equilibrium principle radii as function of the Kelvin radius and thus as a function of relative humidity.

As a second consideration on the size and shape of the condensate the temperature dependence is taken into account. The temperature acts on the Kelvin radius, as does the RH. From (2.4) we see that the effect of temperature on r_K is much less than the effect of humidity. A change in RH from 50% to 51% raises the Kelvin radius by 3%. For this increase of the Kelvin radius a temperature decrease of 8.5 K from room temperature would be needed.

Thirdly, the effect of the spacing between tip and sample is considered. For

[3]The tip is considered to be spherical.

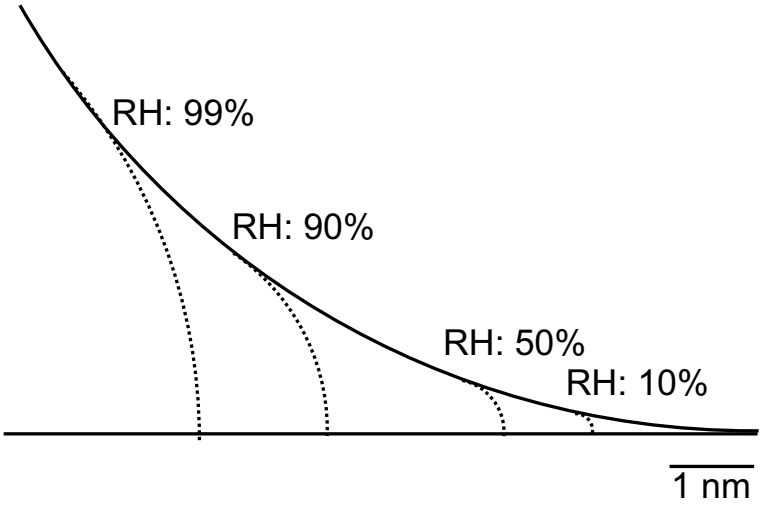

Figure 2.4: The equilibrium shape of one half of the water condensate at RH of 10 %, 50 %, 90 % and 99 %.

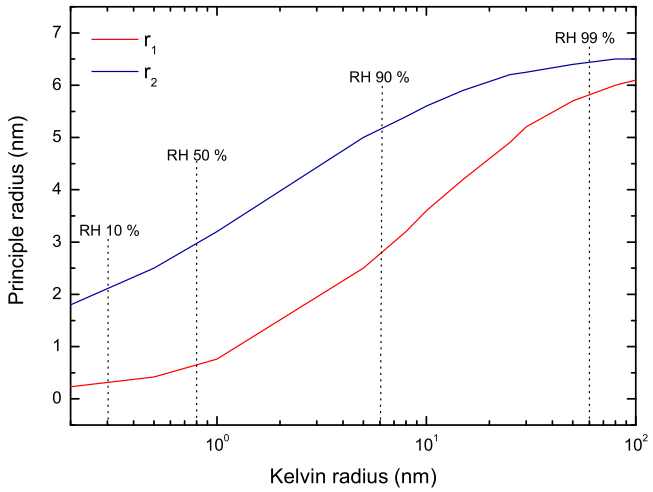

Figure 2.5: Absolute values of the principle radii r_1 and r_2 as function of the absolute value of the Kelvin radius r_K, for $d = 0$ nm, $r_{tip} = 10$ nm and T $= 293$ K.

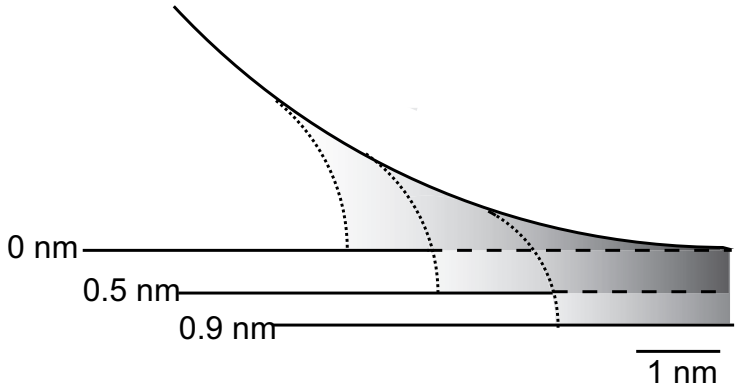

Figure 2.6: The equilibrium shape of one half of the water condensate for d = 0 nm, 0.5 nm and 0.9 nm.

a relative humidity of 90 % and tip radius of 10 nm we vary the spacing d. The resulting water meniscus shape is depicted in Figure 2.6 for three values of d. The effect of increasing d is that the condensate narrows, r_2 decreases and following (2.4), so does r_1, up to the point where no condensate can be stabilized. Obviously, the maximum spacing d_{max} depends on RH; for higher RH, d_{max} is larger; see Figure 2.7 for the effect of spacing for RH of 50% and 90%.

Finally, we take into consideration the effect of the tip radius on the capillary condensation, letting the tip-sample spacing be 0 and the RH 90 %. Figure 2.8 depicts the stable condensate for tip radii of 5 nm and 10 nm and Figure 2.9 shows the dependency of the stable principle radii on the radius of the tip. In the limit of $r_{tip} \to \infty$ we have essentially condensation between two parallel plates and r_1 necessarily approaches the Kelvin radius, as r_2, and thereby the volume of the condensate, may grow indefinitely.

In conclusion, the mechanism is straightforward: at higher humidities larger condensates are stabilized for larger possible values of the tip-sample separation. However, there exists a limit for the dimensions of the condensate when the Kelvin radius approaches infinity at very high values of the RH. Furthermore, a blunter tip can stabilize a larger condensate. The maximum separation d_{max} is also larger for a tip having a larger radius; this is indicated in Figure 2.10. The maximum possible spacing, for a infinitely blunt tip, *is* the Kelvin radius. The model presented is this section is a continuum model using the bulk properties of water. Naturally, at very small length scales this model will fail.

2.1.4 Kinetics of capillary condensation

Up to this point we have addressed the phenomenon of capillary condensation in equilibrium only. Since in scanning probe microscopy the tip is moving with

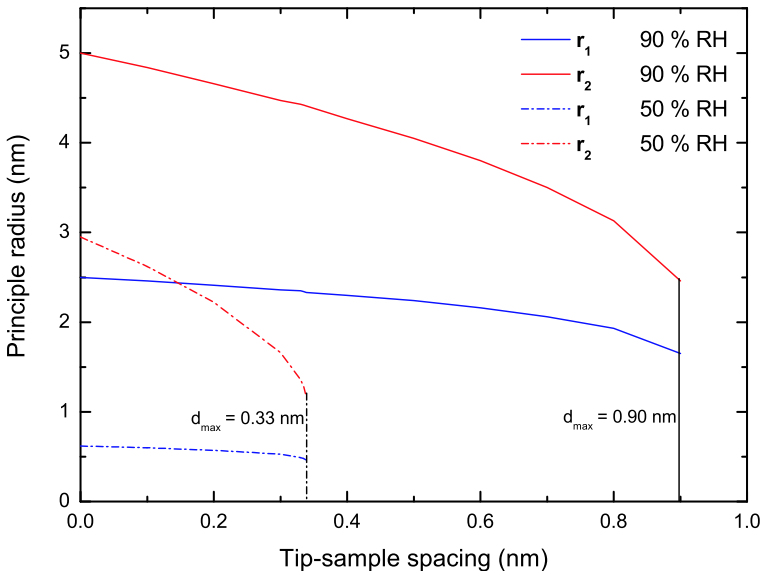

Figure 2.7: Absolute values of the principle radii as a function of the tip-sample spacing for 50 % and 90 % RH. The maximum separation d_{max} is also indicated.

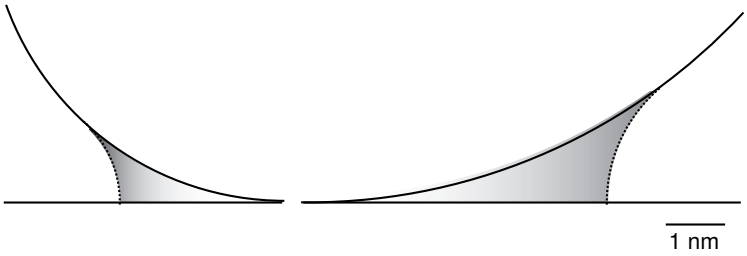

Figure 2.8: *Left*: capillary condensation for $r_{tip} = 5$ nm and *right*: for $r_{tip} = 10$ nm. RH $=$ 90 % and $d = 0$ nm.

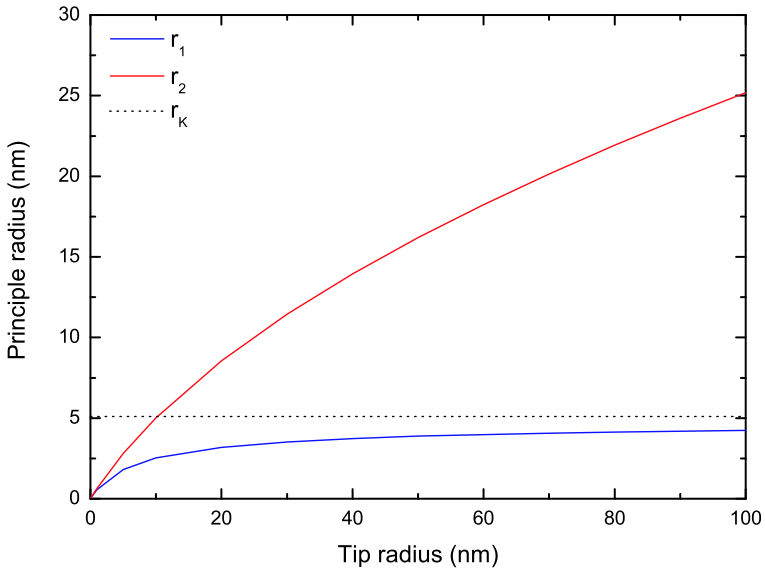

Figure 2.9: The effect of the tip radius on the dimensions of the capillary condensate. RH: 90 % and $d = 0$ nm

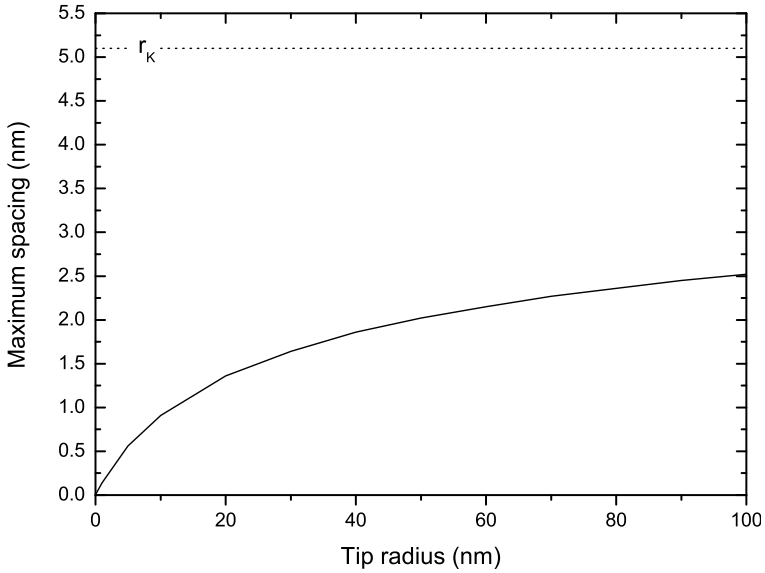

Figure 2.10: The effect of the tip radius on the value of maximum tip-sample spacing. RH is 90 %.

respect to the surface, we must consider the relevant nucleation timescales for condensation of water. The tip is moving in a scanning manner parallel to the surface; in tapping mode (TM) AFM the tip is also oscillating in a plane perpendicular to the surface.

It is suggested [10] that capillary condensation is a thermally activated first order phase transition from the gas to the liquid phase; consequently the nucleation time τ follows an Arrhenius law:

$$\tau = \tau_0 \exp(\Delta E_n / k_B T), \tag{2.7}$$

where E_n is the energy barrier for the nucleation and τ_0 is the attempt period. The nucleation time, for experimental conditions similar to ours, has been determined, with friction force microscopy [11] ranging from 0.7 ms for a temperature of 332 K to 4.2 ms at 299 K. Incidentally, the energy barrier was determined to be 7.8×10^{-20} J and the attempt period to range from 4 ps to 250 ps. It should be noted that the nucleation timescales presented here are still a matter of debate.

2.2 Nanoscale condensates

The present section deals with the properties of nanoscale water clusters, nucleated through the mechanism of capillary condensation, when the scanning probe is no longer present. We will not consider the mechanism of nucleation further, assuming only that the presence of a small confinement served as a nucleation site for a nanoscale cluster. We must, however, consider the nature of the condensate. In the process of capillary condensation we know from (2.1) that the pressure inside the condensate may become negative, which could cause a freezing transition as water expands upon solidifying. As an extreme case, for a rough estimate on the stability of the condensate we take the condensate to be solid and calculate its expected lifetime.

For bulk ice, the sublimation rate at 25°C is 160 mol/(m^2 s), extrapolated from [12]. The impingement rate I, the number of molecules arriving at the surface per unit area and per unit time, is given by:

$$I = \frac{P}{\sqrt{2\pi m k_B T}} \tag{2.8}$$

The impingement rate ranges from 0 to 200 mol/(m^2 s) for 0 to 100% RH. If we have a small, cylinder shaped, cluster of ice on the surface, 100 nm in diameter and 10 nm in height, at 50% RH, the expected lifetime would be 10 μs.

In the calculation above the water is assumed to have bulk properties, which is not evident and the role of the substrate, graphite (hydrophobic) in our case,

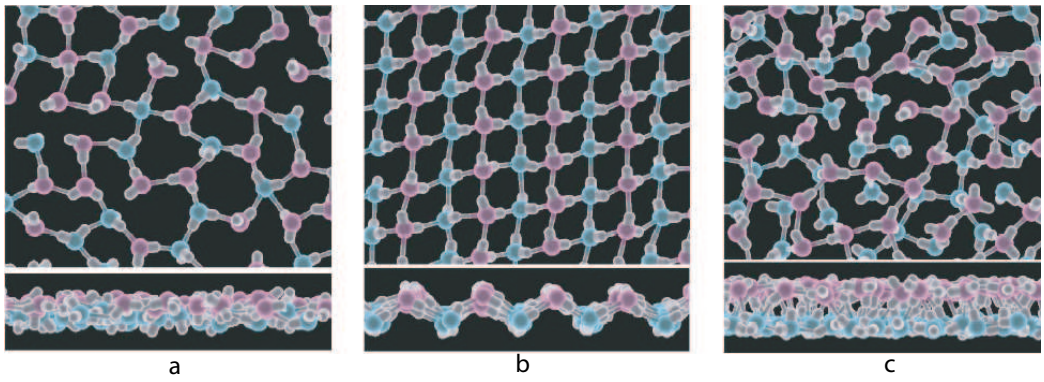

Figure 2.11: MD snapshots from [14]. Lateral and transverse views of a water monolayer, distance between plates: 0.47 nm (a), an ice monolayer, distance: 0.53 nm (b) and a water bilayer, distance: 0.58 nm (c).

is neglected. In fact molecular dynamics (MD) simulation [13] show anomalous density fluctuations (from $0.5\rho_{bulk}$ to $2.8\rho_{bulk}$) up to a distance of 0.8 nm from the water-graphite interface into a nanoscale cluster, with $r = 3$ nm. In this region layering of the water is also observed. Other MD simulations [14] show a first order freezing transition at 300 K of confined water between to parallel plates of quartz (hydrophilic) upon separation of the plates from 0.4 nm to 0.5 nm, see Figure 2.11. Choi *et al.* [15] report a *freezing transition of interfacial water at room temperature under electric fields* for electric fields three orders of magnitude lower than the anticipated electric field needed to align water dipoles for crystallization into polar cubic ice. This work was done in a scanning tunnelling microscopy setup on Au(111)(hydrophilic) using an Au-tip.

On the surface of muscovite mica (hydrophilic), icelike water monolayers at 90% RH have been identified at room temperature using scanning polarization force microscopy (SPFM) [16] in accordance with MD simulations [17]. In another experiment with SPFM [18], the researchers image a graphite surface after a macroscopic drop of a KOH solution was removed with a filter paper. Droplets ranging in size from 10 nm to a fraction of a μm, decorated the steps. Droplets on the same step seemed to have similar sizes. AFM research on graphite surfaces indicated patches of water, 2 and 5 nm typically in height, appearing at high humidity ($>$ 90%), which remained stable for hours when the RH was lowered to less than 1% [19].

The FFM experiments on graphite [6], already mentioned in Chapter1, show the formation of a stripe of ice on the surface, which is present for a characteristic time of 2 s. The ice has an elastic modulus of 2% of the corresponding value for bulk hexagonal ice, which is of the same order of the experimental obtained elastic modulus of a 0.8 nm confined ice layer [20]. The surface force apparatus

(SFA) experiments on a confinement of hydrophobic and hydrophilic surfaces [21] indicate that the confined water has elastic and viscous properties, intermediate to those of bulk liquid water and bulk ice. Equally interesting from this research is the prediction of a ultrathin vapor gap between the hydrophobic surface and the water, which is confirmed in [22]. Here neutron reflectivity measurements show a decrease in water density, near a hydrophobic surface, immersed in water.

From the examples presented it is not to be expected that a nanoscale water cluster has bulk properties, nor that the substrate may be neglected. The calculated time of sublimation is based on a correspondingly naive assumption. What exactly is the nature of the condensate remains a matter of debate, hopefully future measurements on its thermodynamic and mechanical properties, can shed some light upon.

Chapter 3

Experimental results

This chapter presents the experimental results obtained in our research, preceded by a description of the experimental setup. It serves to give an overview of all the data obtained, the analysis being carried out in Chapter 4.

3.1 Experimental setup

The experiments were carried out on two commercial atomic force microscopes, viz. the Digital Instruments Nanoscope IIIa™ and the PicoScan™ of Molecular Imaging Corp., in the following addressed as DI and MI respectively. The AFM tips used were rectangular silicon tips with a normal spring constant of 2 N/m used either in contact mode (CM) or tapping mode (TM). The graphite samples used were highly orientated pyrolytic graphite (HOPG), with supermicrometer grain size. They were cleaved[1] prior to an experimental session

The humidity was controlled by blowing dry nitrogen gas into the environmental chamber to lower the humidity. To raise the humidity the gas was first passed through distilled water before admittance to the environmental chamber. In all experiments, where the temperature was not actively controlled, the temperature was 22°C to 24°C.

[1] Because of the layered structure of graphite it is possible to remove a number of layers in order to obtain a clean and flat sample.

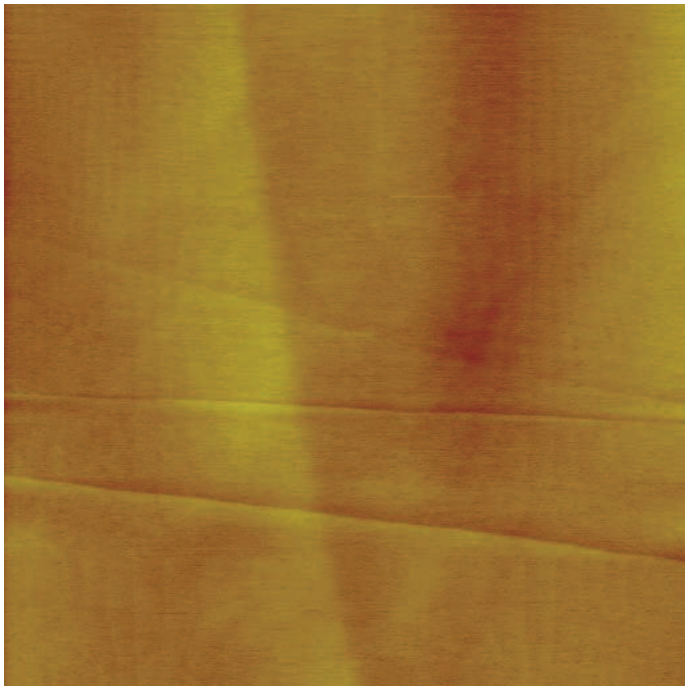

Figure 3.1: TM height image: 4×4 μm^2. Lighter colors indicate higher regions. The 'clean' HOPG surface; showing single atomic steps of 0.3 nm height and multiples thereof

3.2 An overview of the experimental results

Session 1 (DI) In this session the HOPG surface was probed with TM AFM. The surface was imaged at the start of the experiment at room humidity of 30%. Figure 3.1 shows the resulting image. While scanning the RH was continuously raised to a peak value of 95%. At these environmental conditions the observations depicted in Figure 3.2 were done. The creation of a condensate, 3 nm in height[2] and 35 nm in diameter, is shown. After two frames of imaging it becomes stable and was imaged for many frames onward, reducing in height to 2 nm, keeping its original diameter, in 15 minutes time. During this period the RH decreased to 50%. It did not disappear during this session, which lasted 150 minutes after the first capture of the condensate, even when the RH was lowered to less than 10%. At some point, while imagining the condensate and correcting for drift, at a humidity of 10%, a second condensate was visible, appearing at the bottom of the image. The height of this second feature was 1.8 nm, its diameter 30 nm. Figure 3.3 shows four consecutive images of the two condensates, also showing their alignment on some sort of surface feature, appearing as a dim

[2]Actually, it is the apparent height we record, as the interaction potential of tip and sample differs for different materials

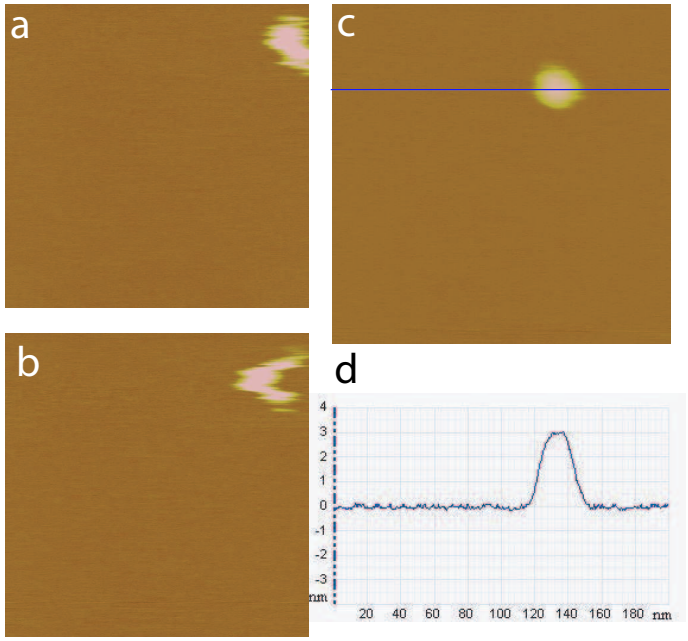

Figure 3.2: Consecutive TM height images: 200×200 nm^2. The creation of the condensate (a) and (b) and the stable condensate (c), with its height profile (d)

line, corresponding to a height of 0.2 nm. This line and the one to the left of it were not visible in Figure 3.2. Furthermore Figure 3.3 shows another shallow feature, 0.2 nm high, moving over the surface from left to right. This can be concluded from the fact that it first appears in Figure 3.3(b), which was captured from top to bottom and then in Figure 3.3(c) captured from bottom to top is under a different angle, to disappear in the next image. Since the images are not snapshots but are recorded in time this feature was moving over the surface under an angle, precisely in between the measured angles, of 82° at a speed of 12 nm/s. Could this be a waterfront, one monolayer thick, moving over the surface?

The session ends with a larger scale overview, showing decoration of surface features, even were the tip had not been scanning before, see Figure 3.4.

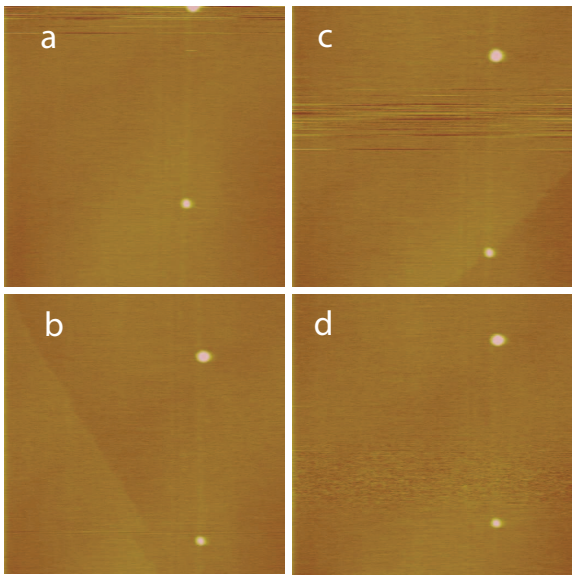

Figure 3.3: Consecutive TM height images: 700×700 nm^2. capture time per image: 50 s. Some drift is visible among the images. In all images two parallel 'lines' are visible, from top to bottom, the right one goes through the condensates. The condensate at the top is the one of Figure 3.2; a new condensate appeared at the bottom (a). The next image, captured from top to bottom, shows a shallow line, of approx. 0.2 nm in height from the upper left corner to the bottom (b), which in the following image (c), captured from bottom to top, runs through the lower feature and disappears in the next image (d).

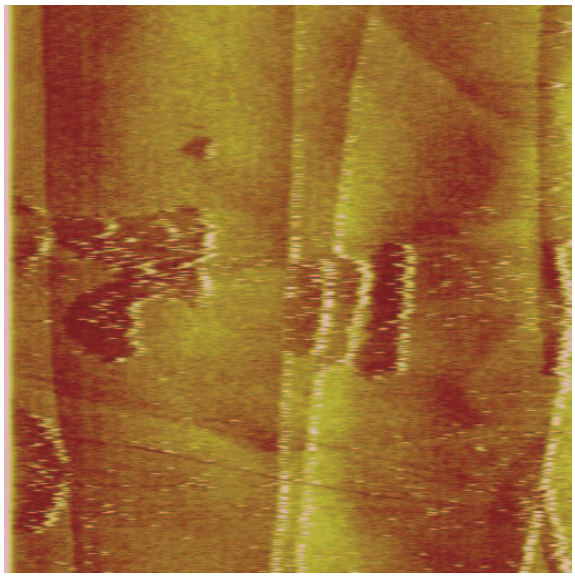

Figure 3.4: TM height image: 10×10 μm^2. The HOPG surface at the end of the experimental session, showing decoration of surface features. The center region, of approximately 3×3 μm^2, is the area that was probed, under high RH conditions in the beginning of the session

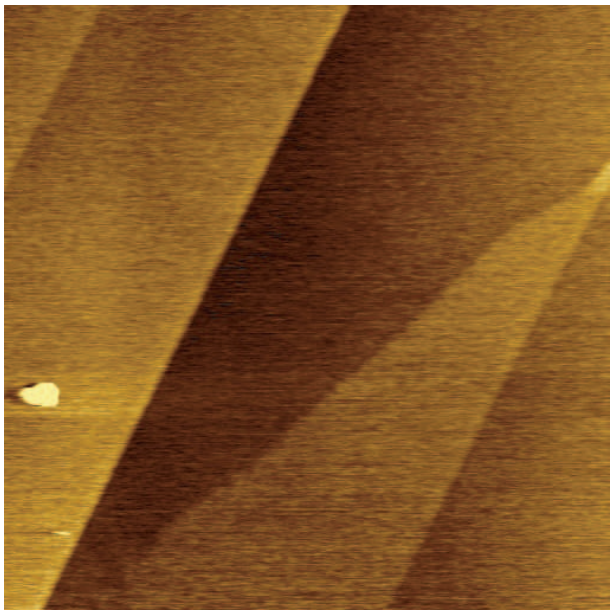

Figure 3.5: TM height image: 5.2×5.2 μm^2. At the start of session 2, the cleaved HOPG shows single atomic and larger steps. The distinct feature in the lower left quadrant is some defilement.

Session 2 (MI) This session was conducted on the MI microscope, operated in TM. Figure 3.5 shows the starting point, taken at 22% RH. As the humidity was increased, already in the next frame the effect is visible, as should be clear from Figure 3.6. This is a distinct difference with session 1 where the nucleation of a single cluster only appeared after some time, seemingly incidental. Still at high humidity an overview image was captured, Figure 3.7, showing the places that had been probed before. Evidence of tip induced nucleation is clearly visible from this. Zooming in on an area, that had already been probed, the observations of Figure 3.8 were recorded.

At this point and on an untouched patch some effort was made to induce nucleation at a specific site of our choice. To this end the tip was placed at a certain position, while it was brought into close contact with the surface. This was done in 'amplitude-to-distance' mode by observing the steep amplitude drop, associated with close contact of tip and sample. The RH was 60%. Figure 3.9 shows the frames captured directly after this. The objects thus created slightly changed their sizes but never fully disappeared, even when the RH was lowered to less than 1%. It was found that no nucleation was possible at this low humidity.

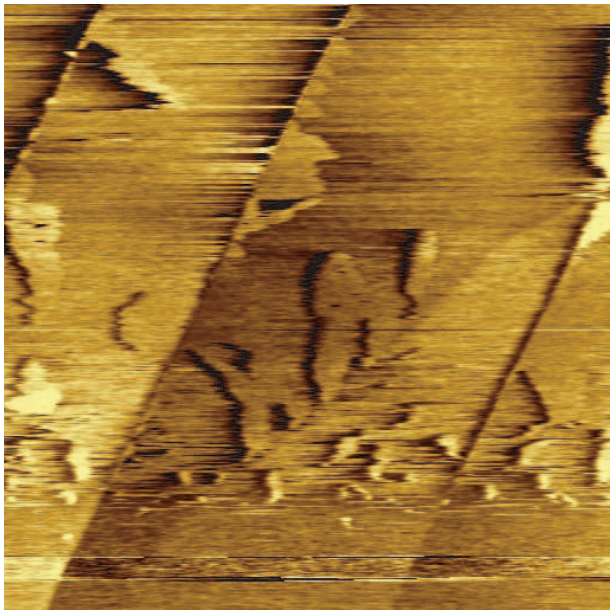

Figure 3.6: TM height image: 5.2×5.2 μm^2. As the RH is raised to 80% the surface appears to be 'flooded'.

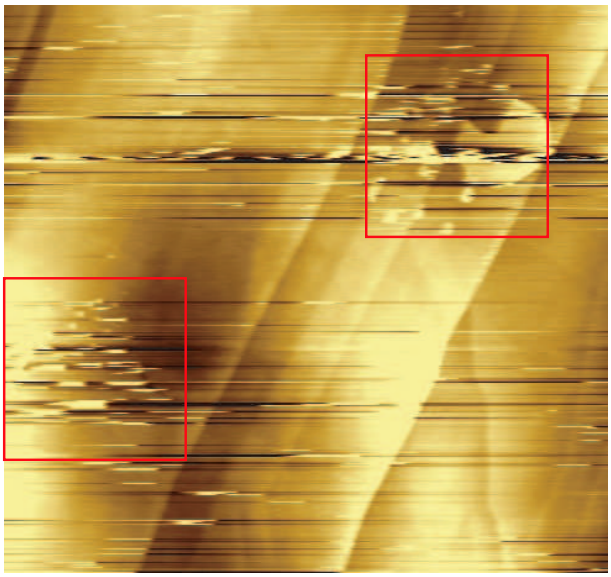

Figure 3.7: TM height image: 46×46 μm^2. Overview image; the red squares indicate previous scan areas.

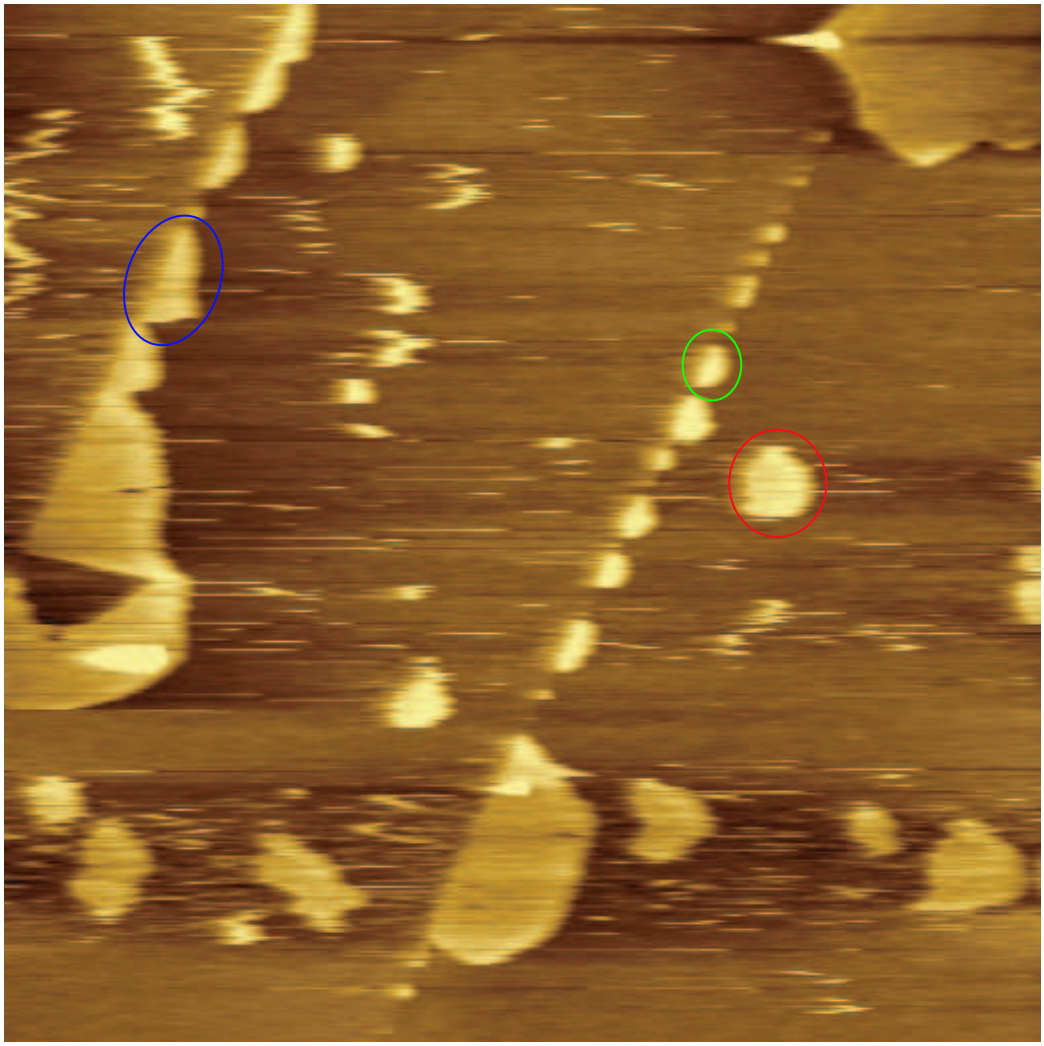

Figure 3.8: TM height image: 5.3×5.3 μm^2. Condensates on the HOPG, imaged at 74% RH. Some features appear to be stable, while others are still blurry. Most of the features have distinct angles and seem to be aligned. To give an idea of the dimensions involved: the red encircled feature is 3.0 nm high and 400 nm wide, the feature encircled in green is 3.5 nm high and 200 nm wide and the blue encircled feature is 2 nm high.

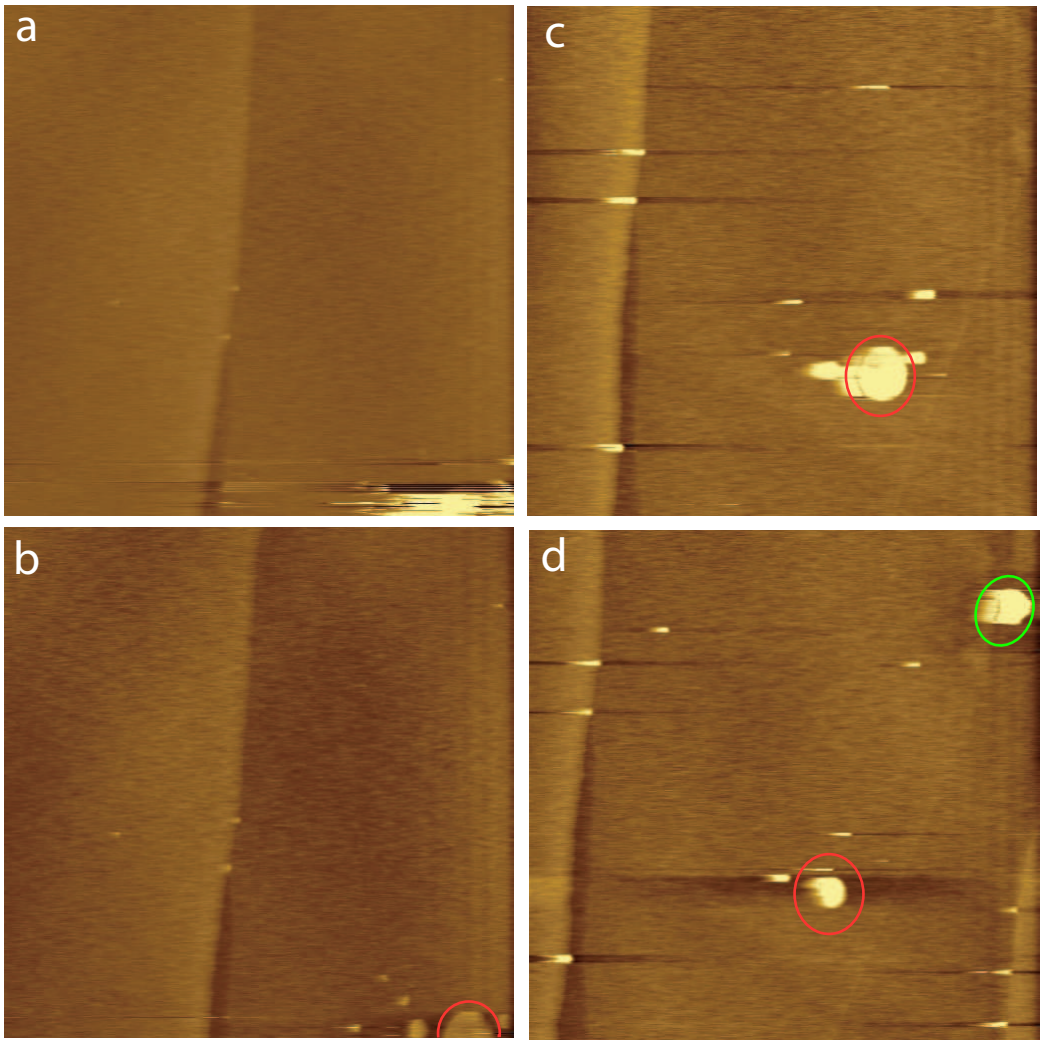

Figure 3.9: TM height images: 7.4×7.4 μm^2. After bringing the tip into close contact with the surface an unstable feature appears at the intended position, at the bottom of the image (a). In the next frame the feature seems to be more distinct in shape (b). Some frames later the feature is more in the center of the picture (c). It is 4.4 nm high. Another feature (encircled green, 5.8 nm high) was intendedly created and the original feature has shrunk in lateral size, maintaining its 4.4 nm height(d).

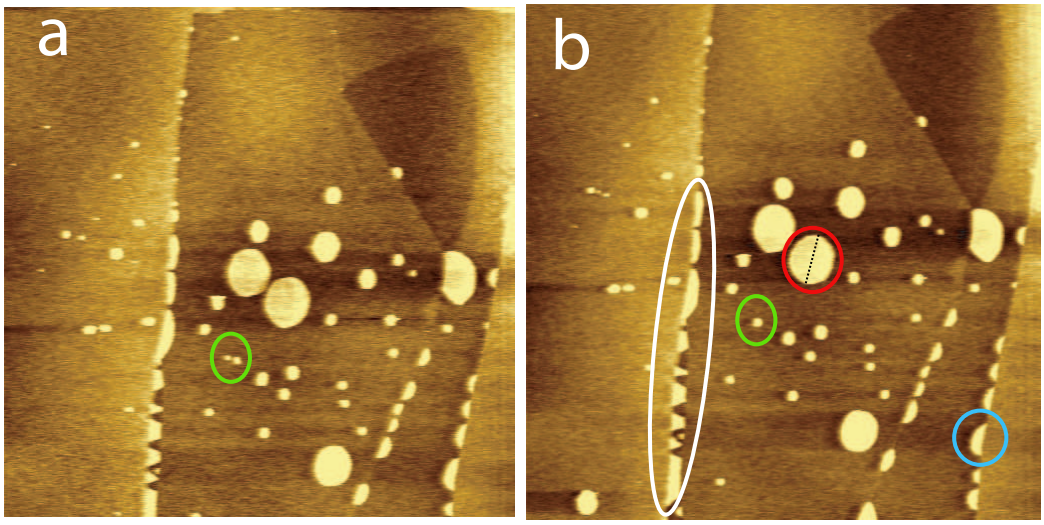

Figure 3.10: TM height images: 10.5×10.5 μm^2. Condensates on the HOPG surface, imaged at 1% RH, among these consecutive images there is one apparent difference located in the green circle. The two features visible in (a) seem to have coalesced in (b), as the feature in (b) is larger then the two separate ones in (a). At the steps, the condensates are situated on the lower terrace, as in the blue circle. This feature, located at a double atomic step (0.6 nm high), is 2.0 nm high (w.r.t. the lower terrace), 750 nm in length along the step and 300 nm at its widest. Another feature (encircled red) is away from a step. Its shape, and that of the condensate to the left of it is not round, rather hexagonal. It is a flat pancake-like structure of 2.0 nm high and 1.0 μm wide, along the dotted line. The features, which are encircled in white, seem to be located in some sort of 'gorge', and have distinct angles.

Session 3 (MI) With the same tip experiments were continued on the MI, after the HOPG sample was cleaved again. The start was at low humidity again, before increasing the RH to 60%, where nucleation occurred. Then the humidity was lowered to less than 1%. The created objects, showing in Figure 3.10, were then stable for several hours on end. The setup was left overnight, with the tip retracted, at 1% RH. The image of Figure 3.11 was captured the next day, 13 hours later. From this picture, the last of this session, the influence of the presence of the tip is clear, as only the center region was probed under high humidity conditions. Some small specks show in the figure, possibly indicating that some drying process occurred, leaving behind some non-volatile material. The features have also become more shallow and some disappeared altogether.

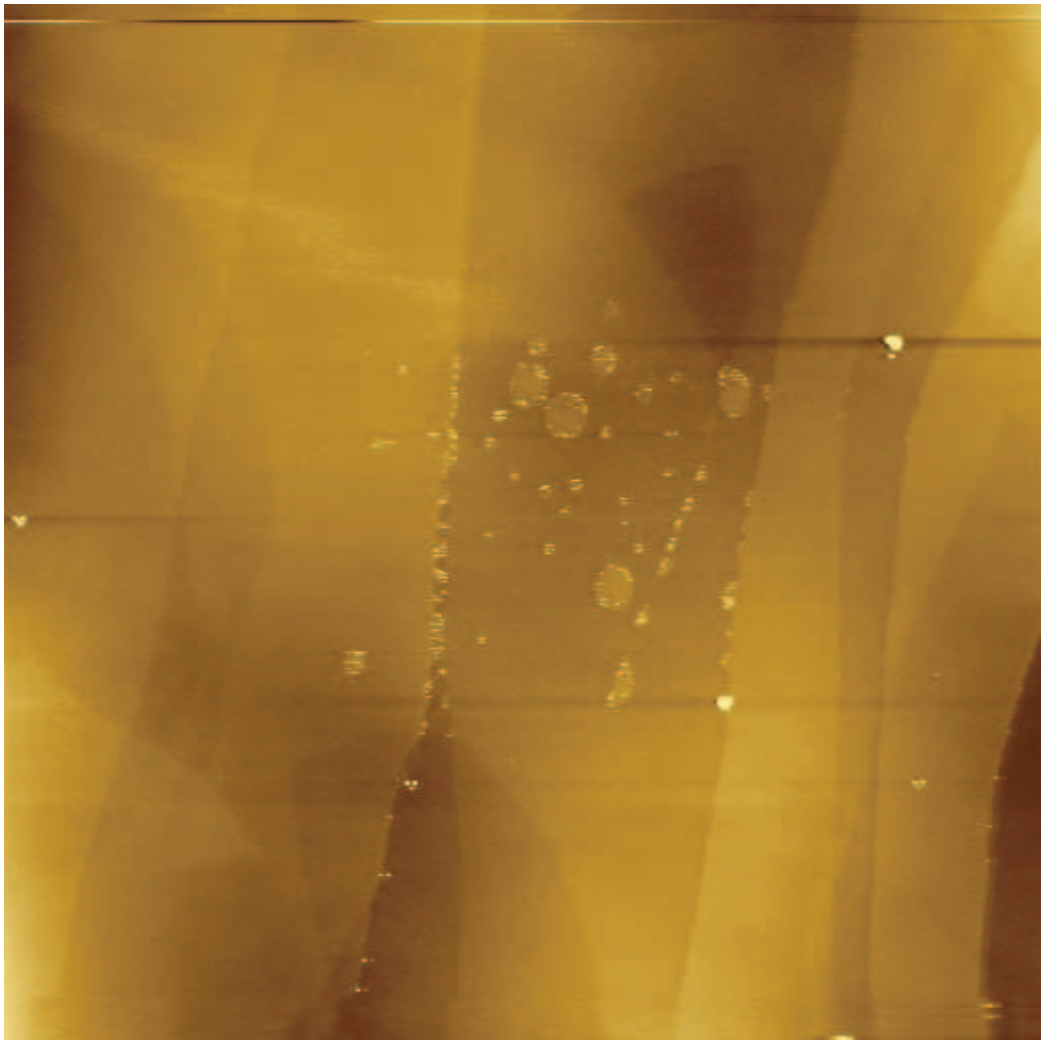

Figure 3.11: TM height image: 21.2×21.2 μm^2. The HOPG surface 13 hours after it had been probed at high humidity. Showing clearly the region scanned before in the middle of the image. The feature, which was encircled in red in Figure 3.10(b), now is 1 nm high and still of the same lateral dimensions. There are also some small specks visible, near the edges of the features.

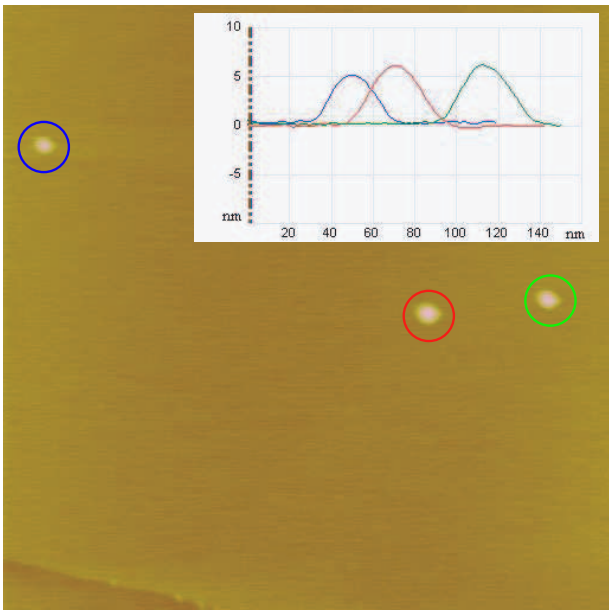

Figure 3.12: TM height image: 1×1 μm^2. The features visible are nucleated in CM at 50 % RH. A height profile is also given for each of the condensates

Session 4 (DI) In the session presented here, the ability to nucleate at any given place is illustrated. One procedure is as follows: at high humidity, the tip is brought into close contact with the sample in CM at a specific place. Then in TM the condensate is visible at the intended position. Three such created condensates are visible in Figure 3.12, along with their height profiles. It was found that in this session at humidity below 40% no nucleation was possible. Furthermore, we tried to image the condensates in CM, at low humidity. This proved to be impossible. Returning to TM again revealed the seemingly unperturbed condensates again.

On another occasion, two condensates were created in CM and imaged in TM. This was followed by a CM scan of smaller scan range. This experiment revealed the possibility to move the condensates over the surface in CM, as is clear from Figure 3.13.

Another procedure to nucleate at a given position is as follows: while imaging in TM, the drive voltage is lowered to 1-10% of the normal drive voltage, thus lowering the free amplitude considerably. The next step is to lower amplitude set point correspondingly, bringing the tip and sample in close contact. One can then also lower the scan velocity letting the tip proceed gently over the surface, allowing for condensation. Then resetting the parameters for normal TM imaging, the condensate is visible. Figure 3.14 shows the result of such an effort.

It has to be said, that it is a matter of trial and error to get the parameters

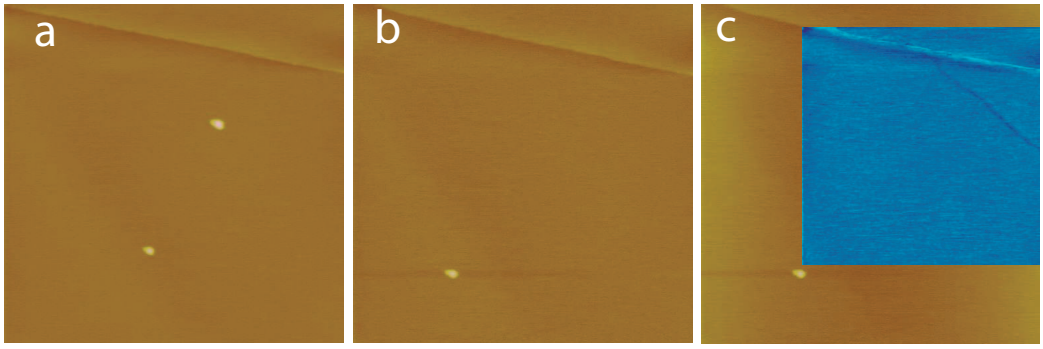

Figure 3.13: TM height images: 1×1 μm^2 (a) and (b) and a composition of TM/CM height image 1×1 μm^2/700×700 nm^2 (c). Two condensates created in CM; the upper one is 5.6 nm high and 55 nm wide, the lower one is 4.2 nm high 46 nm wide (a). Also visible is a double atomic step. The next image (b) is taken right after an attempt to visualize the condensates in CM. Only one condensate is visible (3.9 nm high and 49 nm wide), moved w.r.t. the previous image, the other one disappeared. The same image is overlain with the CM image (blue color scale) resulting in displacement of the condensates (c). It was intended to have the same center in CM imaging as in TM. This was not the case if we assume that the lower condensate was pushed towards the lower left corner in CM, explaining its displacement. The other condensate could then be pushed outside the field of view of 1 μm^2, which is the maximum scan range for the scanner used.

right. It has the advantage over nucleating in CM, though, that one need not need switch modes, thus one need not retract the tip and approach again. This means that it can be done faster and more accurately with respect to the positioning.

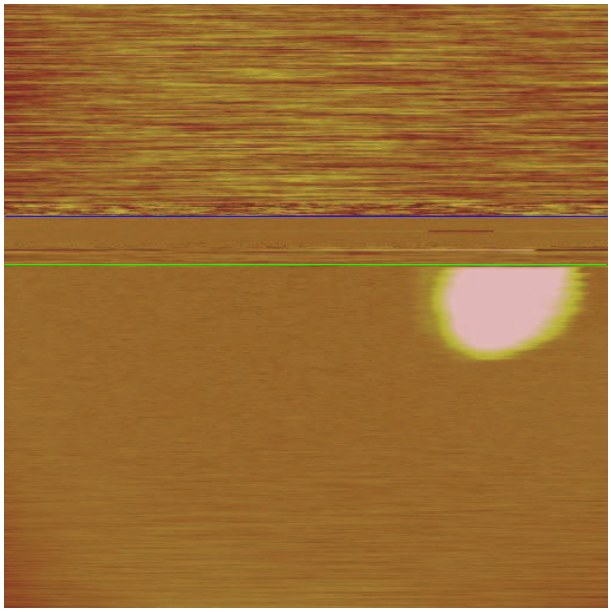

Figure 3.14: TM height image: 160×160 nm^2; scanned from top to bottom. In the region from the top of the image to the blue line the drive voltage was lowered and the tip is out of contact. Between the blue and green lines the amplitude set point is lowered, scanning at 1 line per second. In the lower part of the image the condensate is already visible. It is 8.3 nm high and 42 nm wide

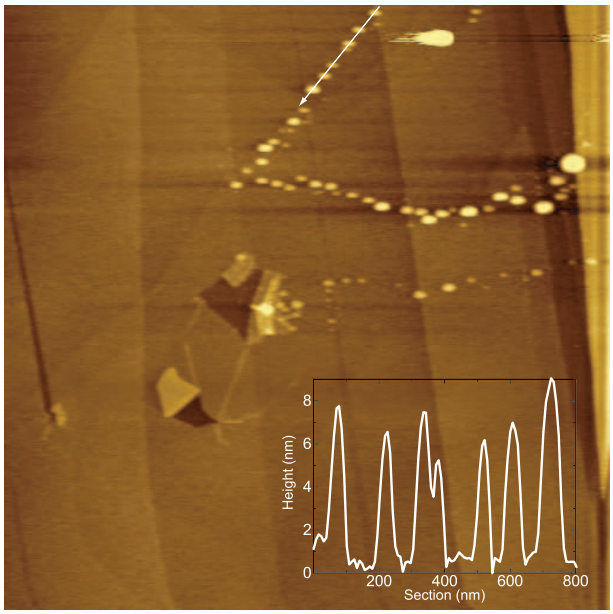

Figure 3.15: TM height image: 4×4 μm^2. The HOPG surface imaged at 11°C (2% RH) after condensation occurred at 9°C (95% RH). There are some features visible on steps. Other features appear to be aligned across terraces. From the upper branch of features an 800 nm height profile is drawn in the direction of the arrow. Furthermore, the surface is damaged, probably from the cleaving process. This clearly shows in two places where the graphite appears to be folded open; the upper damaged region shows condensation on the folded graphite sheets.

Session 5 (MI) With the MI AFM it is possible investigate the influence of temperature on the formation and evolution of the condensates, as it has a sample stage with a Peltier element. Using that, it was possible to vary the temperature from roughly 0°C to 45°C under normal operating conditions[3] and at room temperature (24°C). Although it may seem from the results presented sofar, that condensation occurred at any given trial, this was definitely not the case. Sometimes it was just impossible to nucleate anything on the surface, whatever the humidity was and whatever efforts were done to bring the tip into close contact with the sample.

On three such occasions it was decided to lower the temperature, allowing for a higher probability of nucleation. In all of these instances the temperature was decreased, while the RH was above 90%. The first signs of nucleation occurred respectively for temperatures of 18°C, 13°C and 9°C.

From the last effort the results given in Figure 3.15 were obtained, after the system had come to thermal rest at 11°C. The relative humidity was 2%.

[3]This means that the Peltier element was cooled with water at room temperature and that the electrical current did not exceed the safety limit.

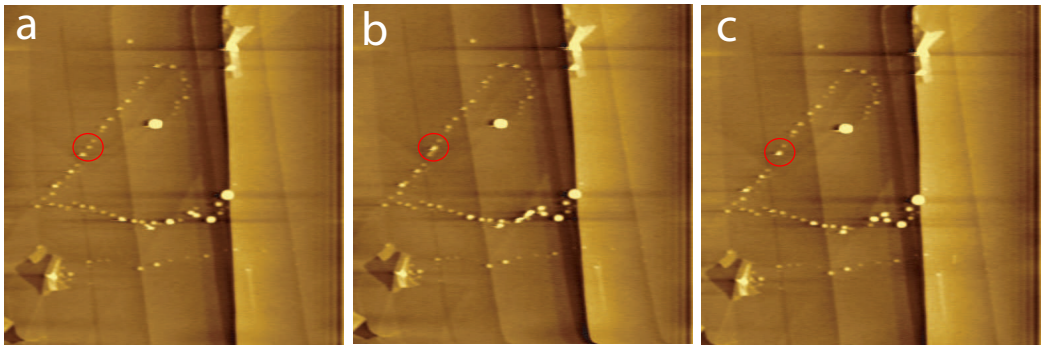

Figure 3.16: TM height images: 4×4 μm^2. Consecutive images showing the coalescence of two condensates, located in the lower part of the red circle. Images captured at RH of 2% and temperature of 31°C.

Maintaining low humidity the temperature was then increased, slowly to minimize thermal drift. At 31°C two condensates seem to coalesce (Figure 3.16). Continuing increasing the temperature more and more condensates disappeared. Figure 3.17 shows the situation at 43°C, which was the highest attainable temperature. After this, the setup was relaxed to room temperature and left overnight, after which is was imaged without any noticeable changes to the surface features.

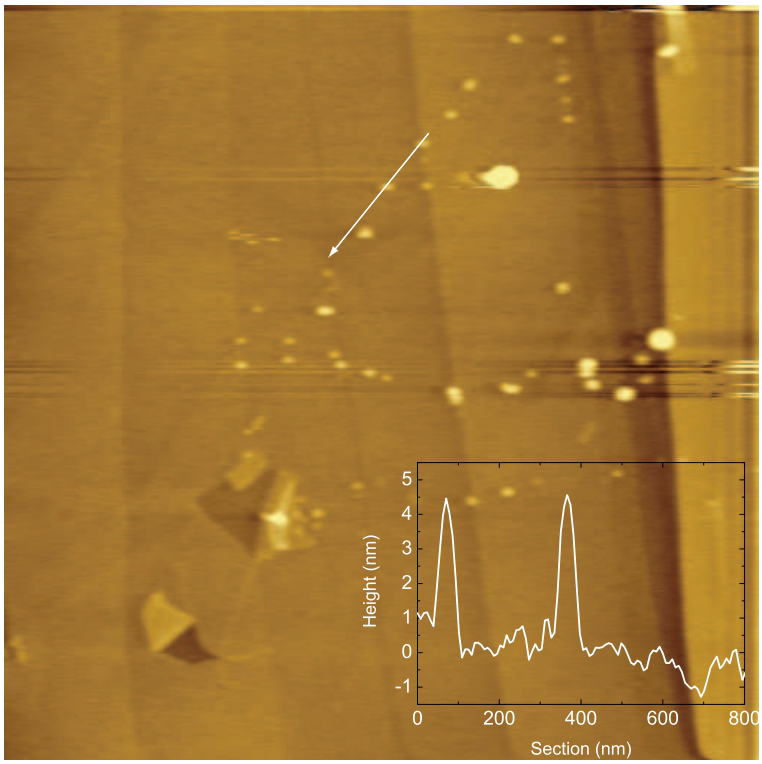

Figure 3.17: TM height image: 4×4 μm^2. The HOPG surface imaged at 43°C (2% RH). With respect to Figure 3.15 some features changed their sizes, some disappeared and others are displaced. The depicted height profile is drawn over the same surface region as in Figure 3.15.

Chapter 4

Discussion & Conclusion

From the results given in the previous chapter it remains unclear what exactly are the properties of the condensates created. We cannot even prove that what we have been imaging *is* water, nor if it is solid or liquid. Efforts to create and image the condensates in a scanning tunnelling microscope setup to enhance the details of the condensates did not succeed. If we assume that it is water in some form, what is perhaps most striking, is the extremely long lifetime of the condensates, which is from thermodynamic calculations, using bulk properties of water, impossible.

As already mentioned in the previous chapter, there certainly was no full reproducibility of our observations. For example the large flat condensates observed in session 3 (Figure 3.10), that had such distinct structures, were only measured once, although many attempts were made. Statistical analysis on the observations to make firm conclusions is hindered by the irreproducibility.

In this chapter we discuss our observations as well as classify the observed condensates to some extend, to end with some concluding remarks.

4.1 General observations

We can make these objective remarks:

- We only managed to nucleate at high RH, above 55-60%.
- It is possible to nucleate the condensates in TM, just by raising the RH. In this case the condensates seem to be positioned at preferential sites. For example, situated on steps in the graphite surface, on the lower terrace or aligned across a terrace, where there was no direct evidence of the underlying surface having special properties. There is clear evidence that the presence of the tip enhances the chance of nucleation, although some

condensation took place where the tip had not been scanning under humid conditions.

- Even when RH is lowered the condensates are present for extremely long times. In most cases their is no or little sign of evaporation although some experimental sessions lasted for over a day.
- In CM it is possible to nucleate at any given position, with reasonable reproducibility. However, the shape and size differ greatly, from session to session.
- It proved to be impossible to visualize the condensates in CM. Returning to TM after such an effort showed that either the condensates were not affected at all, were displaced or had disappeared. The latter could also mean a displacement out of the field-of-view.
- There are also observations of moving a condensate in TM. This usually occurred at higher scan velocities
- There is definitely a temperature effect; in formation as well as evolution of the condensates.

4.2 The size & shape

Our experimental data showed several interesting features on the graphite surface, originating from operation under high RH conditions. Among them are: flat pancake-like structures, curved droplet shaped features, condensates situated on specific sites and possibly a moving water front. In the following we analyze some of the data presented in the previous chapter somewhat more thoroughly.

For the structures of Figure 3.10, that are not placed along steps Figure 4.1 shows the width and height of the condensates. The mean height of 2.2 nm does not seem to depend on the lateral size. The standard deviation in height is 0.3 nm. Some condensates are hexagonally shaped, possibly a sign of crystallization of water.

In the lower right quadrant of Figure 3.10 we observe the condensates to be situated at a step edge, on the lower terrace. This is an indication that truncated graphite layers, from the upper terrace, allow for the bonding of the water.

Also in in Figure 3.10, in the lower left quadrant, a 'gorge' is situated which partly is filled with water. This gorge is 1.0 nm deep w.r.t. the left terrace and 0.7 nm deep w.r.t. the right terrace. From the contact area of the material in the gorge with the sides, it seems that the water is preferably attached to the highest ridge. An explanation for this could be that at one point, at high RH,

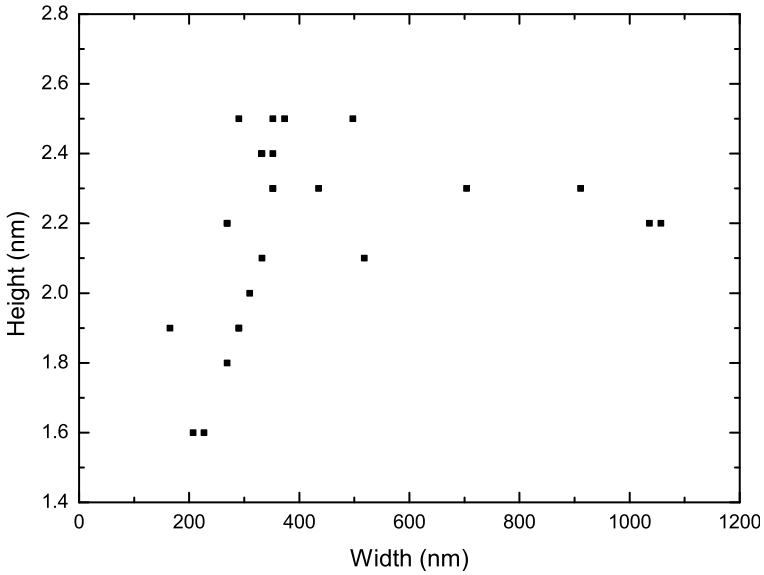

Figure 4.1: A scatterplot of the width and height of the condensates of Figure 3.10 that do not lie on step edges.

the gorge was filled up completely and that when the RH was lowered, the water took this configuration having the majority of its material at the higher terrace to make the most bonds with graphite.

Next we consider the condensates created in experimental session 5, where we varied the temperature of the sample. For the condensates in Figure 3.15, the width and height are shown in Figure 4.2, from which we may deduct the following. There is a positive correlation between the dimensions of the condensates, with R^2 of 0.83[1]. If we model the condensates to be shaped as a spherical cap, we can retrieve the contact angle θ between the condensate and the HOPG substrate, from the ratio of height h and width w:

$$\theta = 90^\circ - \arctan(w/h - h/w), \tag{4.1}$$

using the geometry of Figure 4.3. Evidently, the contact angle should then be the same for every condensate, which implies that the fitted line should go trough the origin of the graph. The reason it does not, could be that, since the tip has a finite size, convolution of tip and imaged sample broadens the features. For instance a very sharp feature on the surface would appear as an image of the tip, and hence as the tip is assumed to be spherical, the smallest possible feature size has the width of the tip. In this case, this would mean an offset in the measured

[1]The square of the Pearson correlation coefficient is a measure of the degree of correlation between two variables; for $R^2 = 0$ there is no correlation, $R^2 = 1$ implies perfect correlation

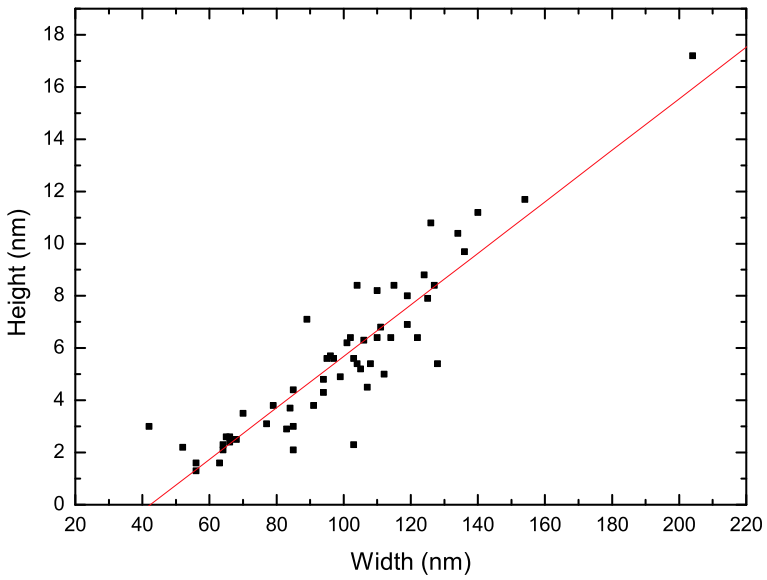

Figure 4.2: A scatterplot of the width and height of the condensates of Figure 3.15.

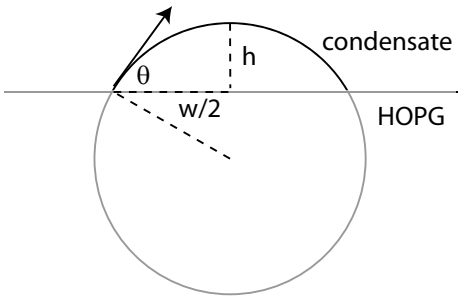

Figure 4.3: Geometry of the condensate on the HOPG surface, assuming it to be shaped as a spherical cap; w is the width of the condensate, h its height.

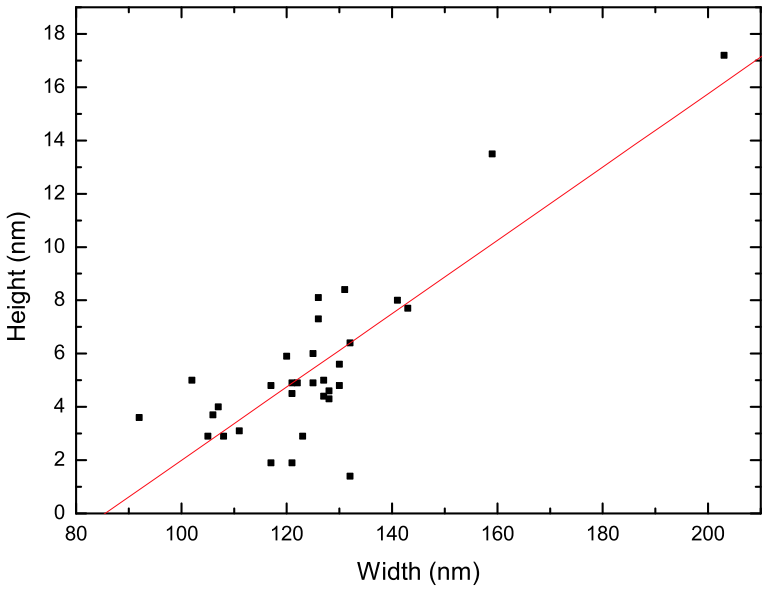

Figure 4.4: A scatterplot of the width and height of the condensates of Figure 3.17.

width of the condensates of 40 nm. Taking this into account, we can take for h/w the slope of the fitted line of 0.10. This leads to a contact angle of $6°$.

In this experimental session, as the temperature was raised, condensates coalesced. An example is depicted in Figure 3.16, where two condensates joined; some frames later the resulting cluster coalesced with yet another condensate. Before the coalescence the three condensates measured 108, 128 and 125 nm in width and 5.4, 5.4 and 7.5 nm in height respectively. The resulting feature is 132 nm wide and 6.4 nm high. Obviously, in this instance, some material disappeared from the surface, during coalescence and heating. If we examine condensates which were not moved during the heating procedure, we find that some shrank and others got larger. The former could be due to evaporation, the latter might be the result of coalescence.

Session 5 was ended at 43 °C with the image of Figure 3.17. The width and height of the condensates ate plotted in Figure 4.4. Now the correlation coefficient R^2 between the dimensions is 0.68, which means that the dimensions are still reasonably well correlated. The interception with the horizontal axis now is 85 nm. If we follow the same argumentation as above on tip-sample convolution, the tip changed its shape and became less sharp. This could be the result of a tip crash with the sample at some point. This is not inconceivable if we bear in mind the large thermal drift, in all directions, during the heating process. The slope of the line, 0.12 for the fit presented, leads to a contact angle of $7°$.

4.3 Conclusion

We have shown that humid conditions in a scanning probe microscope configuration lead to the water condensation on the imaged graphite surface. We did not observe the condensates to have the contact angle of 90° for bulk liquid water on graphite, but a rather smaller value of 6°. The condensates exhibit lifetimes that surpass the anticipated lifetime from thermodynamic considerations by several orders of magnitude. The theory used to describe the condensates, however, is based on the properties of bulk material.

Although, the condensates were situated all over the graphite surface, they were clearly preferably situated along steps. Even when there was no direct sign of the surface providing an ideal site, the apparent alignment of the condensates could hint towards specific surface properties.

During the experiments, the fact that the condensates did not promptly evaporate or sublime, was alarming to such an extend that we had to consider the possibility that what we were imaging was not water but rather some non volatile material. For instance, foreign material, dissolved in the water could reveal itself as a 'drying stain'. This would imply that an environment of high humidity is required to condense the water on the surface and that as the water evaporates it leaves behind the dissolved material. A second consideration was based on the so-called *Dip-pen nanolithography* [23], a technique in which molecules, situated on the AFM tip are transported to the substrate via capillary transport, as in Figure 4.5. In this way, one could leave behind on the surface a structure, that would have a large lifetime.

Our intention was, obviously, to completely rule out these scenarios. To that end we took great care to clean the environment as well as the AFM tip. As we are working in ambient conditions, some degree of pollution is to be expected, however. Yet, from the shape of a large amount of the condensates imaged and presented in this thesis, it is hard to believe that what we are dealing with is some sort of defilement rather than water, be it liquid or solid.

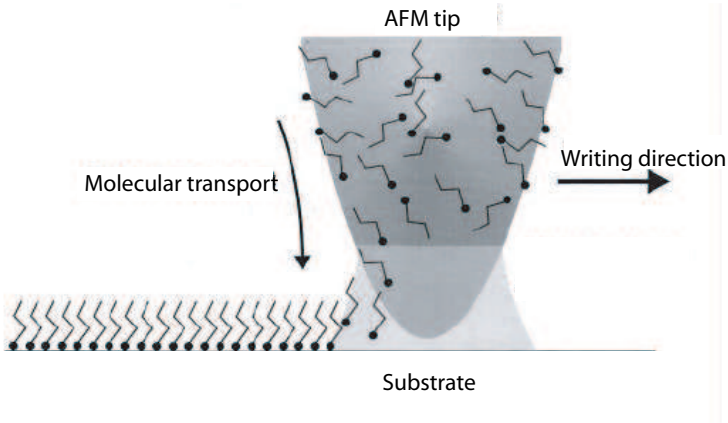

Figure 4.5: The mechanism op dip-pen nanolithography. Under high humid conditions, the AFM tip is in contact with the substrate. A water meniscus serves as a transportation channel for molecules on the tip to travel to the substrate. Figure taken from [23].

The irreproducibility of our observations, as well as the absence of complete understanding of the processes at hand, may be due to the fact that we did not have full control over the experimental parameters. For instance, as is stated in Chapter 2, the sharpness of the tip largely influences the size of the capillary condensate, in a similar way as the RH does and it is not unthinkable that there is some critical size for the condensate to be stable. For future research it is a prerequisite to work in a well defined physical setup in terms cleanliness, tip and sample status and temperature. A thorough investigation on the influence of the latter could shed some light upon the energetics involved as formation and evolution are thermally activated phenomena.

Bibliography

[1] G. Binnig, H. Rohrer, C. Gerber, and F. Scire. *Phys. Rev. Lett.*, 49:57, 1982.

[2] G. Binnig, C. F. Quate, and C. Gerber. *Phys. Rev. Lett.*, 56:930, 1986.

[3] B. Bhushan. *Wear*, 259:1507, 2005.

[4] E. Riedo, F. Lévy, and F. Blume. *Phys. Rev. Lett.*, 88:185505, 2002.

[5] R. R. Zamora, C. M. Sanchez, F. L. Freire Jr., and R. Prioli. *Phys. Stat. Sol.*, 201:850, 2004.

[6] K. B. Jinesh and J. W. M. Frenken. *Phys. Rev. Lett.*, 96:166103, 2006.

[7] M. Dienwiebel *et al. Rev. Sci. Instrum.*, 76:043704, 2005.

[8] J. Israelachvili. *Intermolecular & surface forces*. Elsevier, 1985.

[9] O. Sinanoglu. *Chem. Phys. Lett.*, 81(2):188, 1981.

[10] F. Restango, L. Bocquet, and T. Biben. *Phys. Rev. Lett.*, 84:2433, 2000.

[11] R. Szoszkiewicz and E. Riedo. *Phys. Rev. Lett.*, 95:135502, 2005.

[12] M. Elbaum. *Optical search for melting of ice*. PhD thesis, University of Washington, 1991.

[13] T. Werder, J. H. Walther, R. L. Jaffe, T. Halicioglu, and P. Koumoutsakos. *J. Phys. Chem. B*, 107:1345, 2003.

[14] R. Zangi and A. E. Mark. *Phys. Rev. Lett.*, 91:025502, 2003.

[15] E. M. Choi, Y. H. Yoon, S. Lee, and H. Kang. *Phys. Rev. Lett.*, 95:085701, 2005.

[16] P. B. Miranda, Y. R. Shen L. Xu, and M. Salmeron. *Phys. Rev. Lett.*, 81:5876, 1998.

[17] M. Odelius, M. Bernasconi, and M. Parrinello. *Phys. Rev. Lett.*, 78:2855, 1997.

[18] J. Hu, X. D. Xiao, and M. Salmeron. *Appl. Phys. Lett.*, 67:476, 1995.

[19] A. Gil, M. Luna, J. Gómez, and A. M. Baró. *Langmuir*, 16:5086, 2000.

[20] J. D. Porter and A. S. Zinn-Warner. *Phys. Rev. Lett.*, 21:2879, 1994.

[21] X. Zang, Y. Zhu, and S. Granick. *Science*, 295:663, 2002.

[22] D. Schwendel, T. Hayashi, R. Dahint, A. Pertsin, M. Grunze, R. Steitz, and F. Schreiber. *Langmuir*, 19:2284, 2003.

[23] R. D. Piner, J. Zhu, F. Xu, S. Hong, and C. A. Mirkin. *Science*, 283:661, 1999.

Acknowledgements

During this research project I have benefitted strongly from the theoretical knowledge and practical skills of the *Interface Physics* group. The cooperation in the group and interest in each other's work are a stimulus for creative scientific work.

In particular I would like to thank my supervisors, Tjerk Oosterkamp and Merlijn van Spengen, for guiding the research. I value the discussions on the physics of the surface processes with Joost Frenken highly and enjoyed working with Marcel Rost in an effort to clarify the matter with STM. I thank Maarten van Es for teaching me how to work with an AFM and I really liked working with K. B. Jinesh in the quest for understanding water in our experiments.